Low Energy, Coherent, Stoner-like Excitations in $CaFe_2As_2$

Liqin Ke[1], M. van Schilfgaarde[1], J.J.Pulikkotil[2], T. Kotani[3], and V.P.Antropov[2]

[1] *School of Materials, Arizona State University*

[2] *Ames Laboratory, IA 50011 and*

[3] *Tottori University, Tottori, Japan*

(Dated: June 30, 2010)

Abstract

Using linear-response density-functional theory, magnetic excitations in the striped phase of $CaFe_2As_2$ are studied as a function of local moment amplitude. We find a new kind of excitation: sharp resonances of Stoner-like (itinerant) excitations at energies comparable to the Néel temperature, originating largely from a narrow band of Fe d states near the Fermi level, and coexist with more conventional (localized) spin waves. Both kinds of excitations can show multiple branches, highlighting the inadequacy of a description based on a localized spin model.

Magnetic interactions are likely to play a key role in mediating superconductivity in the recently discovered family of iron pnictides; yet their character is not yet well understood. In particular, whether the system is best described in terms of large, local magnetic moments centered at each Fe site, in which case elementary excitations are collective spin waves (SWs) called magnons, or is itinerant (elementary excitations characterized by single particle electron-hole transitions) is a subject of great debate. This classification also depends on the energy scale of interest. The most relevant energy scale in $CaFe_2As_2$ and other pnictides ranges to about twice the Néel temperature, $2T_N{\approx}40$ meV. Unfortunately, neutron scattering experiments have focused on the character of excitations in the 150-200 meV range [1, 2], much larger than energy that stabilizes observed magnetism or superconductivity. Experiments in Refs. [1, 2], while very similar, take completely different points of view concerning the magnetic excitations they observe. There is a similar dichotomy in theoretical analyses of magnetic interactions[3, 4]. Model descriptions usually postulate a local-moments picture [5]. Most *ab initio* studies start from the local spin-density approximation (LSDA) to density functional theory. While the LSDA traditionally favors itinerant magnetism (weak on-site Coulomb correlations), practitioners strongly disagree about the character of pnictides; indeed the same results are used as a proof of both localized and itinerant descriptions [3, 4].

The dynamic magnetic susceptibility (DMS), is the central quantity that uniquely characterizes magnetic excitations. It can elucidate the origins of magnetic interactions and distinguish between localized and itinerant character. However, the dynamical linear response is very difficult to carry out computationally; studies to date been limited to a few simple systems. Here we adapt an all-electron linear response technique developed recently [6, 7] to calculate the transverse DMS, $\chi(\mathbf{q},\omega)$. Besides SW excitations seen in neutron scattering, we find low energy particle-hole excitations at low q, and also at high q. In stark contrast to conventional particle-hole excitations in the Stoner continuum, they can be sharply peaked in energy (resonances) and can be measured.

The full transverse DMS $\chi(\mathbf{r},\mathbf{r}',\mathbf{q},\omega)$ is a function of coordinates $\mathbf{r}$ and $\mathbf{r}'$ (confined to the unit cell). It is obtained from the non-interacting susceptibility $\chi_0(\mathbf{r},\mathbf{r}',\mathbf{q},\omega)$ via the standard relation [8]

$$\chi = \chi_0 \left[1 - \chi_0 I\right]^{-1} \tag{1}$$

I is the exchange-correlation kernel. When computed within the time-dependent LSDA

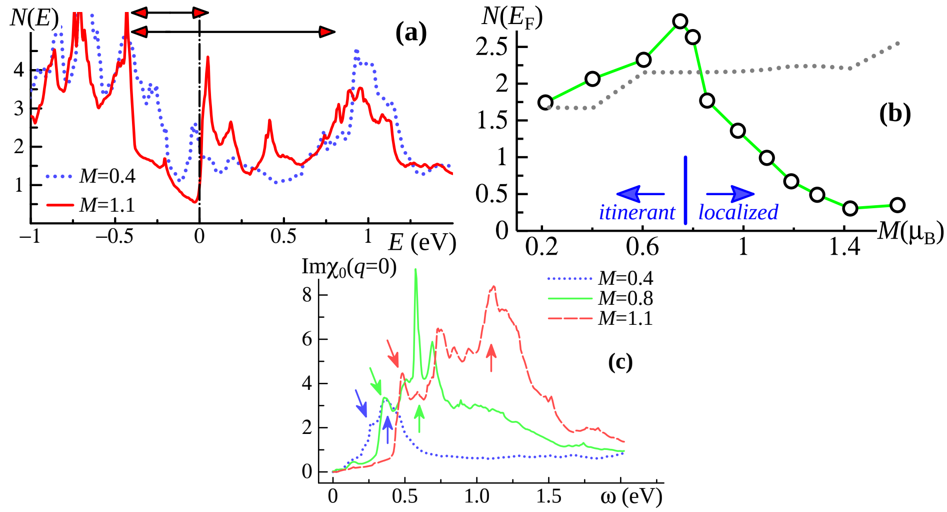

FIG. 1: (**a**) $N(E)$, in units of eV^{-1} per cell containing one Fe atom. Data are shown for M=0.4μ_B and 1.1μ_B. Both kinds of transitions are reflected in peaks in $\chi_0(q{=}0,\omega)$, shown in panel (**c**) for M=0.4, 0.8, and 1.1μ_B. (**b**) $N(E)$ at the Fermi level E_F as a function of moment M. The blue vertical bar denotes the experimental moment, and also approximately demarcates the transition from itinerant to localized behavior. $N(E_F)$ in the nonmagnetic case is shown as a dotted line. (**c**) bare susceptibility $\chi_0(q{=}0,\omega)$ in the same units. The text discusses the significance of the arrows in panels (**a**) and (**c**).

(TDLDA) I is local: $I{=}I(\mathbf{r})\delta(\mathbf{r}-\mathbf{r}')$ [8]. χ_0 can be obtained from the band structure using the all-electron methodology we developed [6, 7]. To reduce the computational cost we calculate Imχ_0 and obtain Reχ_0 from the Kramers Kronig transformation [6]. Imχ_0 originates from spin-flip transitions between occupied states at $\mathbf{k}$ and unoccupied states at $\mathbf{k}+\mathbf{q}$: it is a k-resolved joint density of states D decorated by products P of four wave functions [7]

$$D(\mathbf{k},\mathbf{q},\omega) = f(\epsilon^{\uparrow}_{\mathbf{k}})(1-f(\epsilon^{\downarrow}_{\mathbf{q+k}}))\delta(\omega-\epsilon^{\downarrow}_{\mathbf{q+k}}+\epsilon^{\uparrow}_{\mathbf{k}}) \tag{2}$$

$$\mathrm{Im}\chi_0^{+-} = \int d\omega d^3\mathbf{k} P(\mathbf{r},\mathbf{r}',\mathbf{k},\mathbf{q})\times D(\mathbf{k},\mathbf{q},\omega) \tag{3}$$

Even with the Kramers-Kronig transformation, Eq. (3) poses a huge computational burden for the fine frequency and k resolution required here. We make a simplification, mapping χ_0 onto the local magnetization density which is assumed to rotate rigidly. The full $\chi_0(\mathbf{r},\mathbf{r}',\mathbf{q},\omega)$ simplifies to the discrete matrix $\chi_0(\mathbf{R},\mathbf{R}',\mathbf{q},\omega)$ associated with pairs of magnetic sites $(\mathbf{R},\mathbf{R}')$ in the unit cell; and $I(\mathbf{r})$ simplifies to a diagonal matrix $I_{\mathbf{RR}}$. In Ref. [7]

we show that we need not compute I explicitly but can determine it from a sum rule. I can be identified with the Stoner parameter in models. We have found that for Fe and Ni these approximations yield results in rather good agreement with the full TDLDA results, and expect similar agreement here. We essentially follow the procedure described in detail in Ref. [7], and obtain $\chi(\mathbf{q},\omega)$ as a 4×4 matrix corresponding to the four Fe sites in the unit cell. To make connection with neutron experiments, spectra are obtained from the matrix element $\sum_{\mathbf{R},\mathbf{R}'} < e^{i\mathbf{q}\cdot\mathbf{R}}|\chi(\mathbf{R},\mathbf{R}',\mathbf{q},\omega)|e^{i\mathbf{q}\cdot\mathbf{R}'} >$. For brevity we omit indices $\mathbf{RR}'$ henceforth.

As we will see, the character of $\chi_0(\mathbf{q},\omega)$ can largely be understood from states near E_F, so we begin by analyzing the ground state band and magnetic structure of the low-temperature (striped) phase of $CaFe_2As_2$ within the LSDA. Results for tetragonal and orthorhombic striped structures are very similar, suggesting that the slight difference in measured a and b lattice parameters plays a minor role in the description of magnetic properties. Experimental lattice parameters were employed[9]. $CaFe_2As_2$ has an internal parameter z which determines the Fe-As distance $R_{\mathrm{Fe-As}}$. Here we treat z as a parameter whos main effect is to control the magnetic moment M, which in turn strongly affects the character of magnetic interaction, as we will show.

In Fig. 1(a), the density of states $N(E)$ is shown over a 2 eV energy window for a small and large moment case (M=0.4μ_B and 1.1μ_B). Particularly of note is a sharp peak near E_F, of width ~50 meV. This narrow band is found to consist almost entirely of majority-spin Fe d_{xy} and d_{yz} orbitals. The peak falls slightly below E_F for M=0.4μ_B and slightly above for M=1.1μ_B. Thus, as $R_{\mathrm{Fe-As}}$ is smoothly varied so that M changes continuously, this peak passes through E_F. As a result $N(E_F)$ reaching a maximum around M=0.8μ_B (Fig. 1(b)). This point also coincides with the LSDA minimum-energy value of $R_{\mathrm{Fe-As}}$. That this unusual dependence originates in the magnetic part of the Hamiltonian can be verified by repeating the calculation in the nonmagnetic case. As Fig. 1(b) shows, the nonmagnetic $N(E_F)$ is large, and approximately independent of $R_{\mathrm{Fe-As}}$. In summary, the magnetic splitting produces a pseudogap in $N(E)$ for large M; the pseudogap shrinks as M decreases and causes a narrow band of Fe d states to pass through E_F, creating a sharp maximum in $N(E_F)$ near M=0.8μ_B. As we will show below that moment demarcates a point of transition from itinerant to localized behavior (see also Ref. [13]).

Next we turn to magnetic excitations. In the standard picture of magnons in metals, $\mathrm{Im}\chi_0(\omega)$ is significant only for frequencies exceeding the magnetic (Stoner) splitting of the d

bands, $\epsilon_d^{\downarrow} - \epsilon_d^{\uparrow} = IM$ (*cf* Eq. 2). In such cases Imχ_0 is small at low q and low energies and well defined magnons appear at energies near $|1 - I\mathrm{Re}\chi_0| = 0$ (*cf* Eq. 1). As Imχ_0 increases, it initially broadens the (formerly sharp) SW spectrum $\bar{\omega}(\mathbf{q})$; as it becomes large the spectrum can become incoherent, or (Stoner) peaks can arise from Imχ_0, possibly enhanced by small $1 - I\mathrm{Re}\chi_0$. Fig. 1(c) shows Im$\chi_0(q{=}0, \omega)$ on a broad energy scale. The picture we developed for $N(E)$ leads naturally to a classification of Stoner transitions into three main types.

(1) Excitations between the (largely) Fe d_{xz} states centered near -0.5 eV to d states centered near 1 eV (for $M{=}1.1\mu_B$). The magnetic splitting of these states matches well with the usual Stoner splitting IM in localized magnets, and scales with M. ($I{\approx}1$ eV in $3d$ transition metals.) These high-energy transitions are depicted by a large red arrow in Fig. 1(a) for $M{=}1.1\mu_B$, and by vertical arrows in Fig. 1(c) showing $\chi_0(q{=}0{,}\omega)$ for $M{=}0.4$, 0.8, and $1.1\mu_B$. They are too high in energy to be observed by neutron measurements.

(2) Excitations from d_{xz} to d_{xy} and d_{yz} states just above the psueudogap, depicted by a small red arrow in Fig. 1(a), and slanting arrows in Fig. 1(d). These are the excitations probably detected in neutron measurements [1, 2]. This pseudogap is well defined for $M{\geq}1.1\mu_B$, but is modified as M decreases, which leads to the following:

(3) Near $M{=}0.8\mu_B$, the narrow d band passes through E_F, opening up channels, not previously considered, for low-energy, particle-hole transitions within this band. When M reaches $0.4\mu_B$, this band has mostly passed through E_F and the pseudogap practically disappears.

What makes the pnictide systems so unusual is that Imχ_0 is already large at very low energies (${\sim}10$ meV) once the sharp peak in $N(E)$ approaches E_F. One of our central findings is that this system undergoes a *transition from localized to a coexistence of localized and itinerant behavior* as M decreases from $M{\gtrsim}1.1\mu_B$ to $M{\approx}0.8\mu_B$. Moreover, the itinerant character is of an unusual type: elementary excitations are mostly single particle-hole like: they can be well defined in energy and q. Those represent *coherent* excitations. The dependence of $N(E_F)$ on M is not only responsible for them, but also may explain the unusual linear temperature-dependence of paramagnetic susceptibility, and the appearance of a Lifshitz transition with Co doping [10].

Fig. 2 focuses on the AFM line, $\mathbf{q}{=}[H00]2\pi/a$. Panel (**a**) shows the full Im$\chi(\omega)$ for $M{=}1.1\mu_B$ for several q-points spanning the entire line, $0{<}H{<}1$. At low q, peaks $\bar{\omega}$ in χ are sharp; and $\bar{\omega}$ depends on H in the expected manner ($\bar{\omega}{\propto}H$). $\bar{\omega}$ reaches a maximum

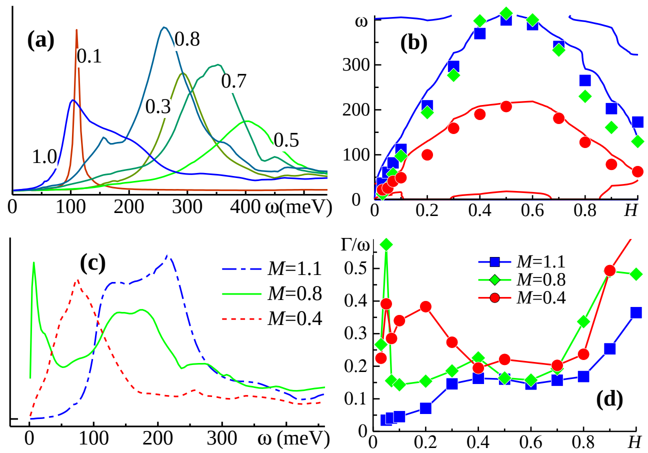

FIG. 2: Im$\chi(\mathbf{q},\omega)$ along the AFM axis, $\mathbf{q}$=[H,0,0]$2\pi/a$. (**a**) Im$\chi(\omega)$ for various H and M=1.1μ_B. Extracted from Im$\chi(H,\omega)$ are peak positions $\bar{\omega}(H)$ (meV) and HWHM Γ. (**b**) and (**d**) depict $\bar{\omega}$ and the ratio $\Gamma/\bar{\omega}$, for the three moments shown in the key. Panel (**b**) also depicts, as solid lines, contours $|1-I\mathrm{Re}\chi_0|=0$ in the (ω,H) plane, for M=1.1 and 0.4μ_B. Panel (**c**) shows Imχ(H=0.9,ω) for the three moments.

near H=1/2 (Fig. 2(b)), for all three values of M. The peaks broaden with increasing q; nevertheless we can associate them with magnons, because they coincide closely with vanishing $|1-I\mathrm{Re}\chi_0|$ and Γ is not too large. The magnon character is preserved for most q at all moments, as Fig. 2(b) shows: but for H>0.8 the peaks are strongly broadened, especially for small M. $\bar{\omega}$ is in good agreement with neutron data of Ref.[2], except that neutron data are apparently smaller than large M calculations predict [11].

One experimental measure of the validity of the local-moment picture is the ratio of half-width at half-maximum (HWHM) Γ to $\bar{\omega}$, shown in Fig. 2(d). For large M and most of q, $\Gamma/\bar{\omega}$ ~0.15-0.18. For intermediate and small M, $\Gamma/\bar{\omega}$ ≥0.2 for a wide diapason of q. This is significant: it reflects the increasing Stoner character of the elementary excitations. Were there an abrupt transition into a conventional Stoner continuum as argued in Ref. [2], it would be marked by an abrupt change in $\Gamma/\bar{\omega}$. This is not observed; yet damping appears to increase with energy and q, reflecting normal metallic behavior.

Spectra for H=0.9 (Fig. 2(c)) adumbrate two important findings of this work. When M=0.8μ_B, a sharp peak in $\chi(\omega)$ appears near 10 meV. There is a sharp peak in $\chi_0(\omega)$ at $\bar{\omega}$≈10 meV also, classifying this as a particle-hole excitation originating from the narrow d band depicted in Fig. 1. Being well defined in energy it is coherent, analogous to a SW,

only with a much larger $\Gamma/\bar{\omega}$. Yet it is strongly enhanced by collective interactions, since $|1-I\mathrm{Re}\chi_0|$ ranges between 0.1 and 0.2 for ω<100 meV. This new kind of itinerant excitation will be seen at many values q, typically at small q. The reader many note the sharp rise and fall in $\Gamma/\bar{\omega}$ at small q in Fig. 2(d). This anomaly reflects a point where a SW and a particle-hole excitation coalesce to the same $\bar{\omega}$.

Returning to H=0.9 when M=1.1, there is a standard (broadened) SW at 200 meV; *cf* contours in Fig. 2(b). A *second*, low-energy excitation can be resolved near 120 meV. This is no corresponding zero in the denominator in Eq. (1), but no strong peak in $\chi_0(\omega)$, either. This excitation must be classified as a hybrid intermediate between Stoner excitations and SWs. Only a single peak remains when M=0.4μ_B and the peak in $N(E)$ has mostly passed through E_F (Fig. 1).

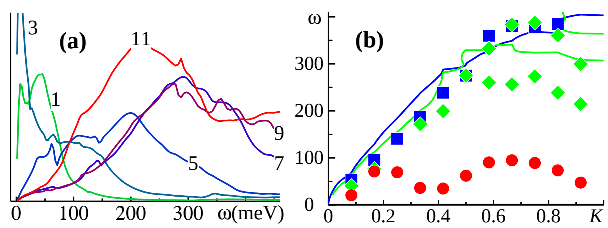

FIG. 3: Im$\chi(\mathbf{q},\omega)$ along the FM axis, $\mathbf{q}$=[0,K,0]$2\pi/a$. (**a**) Im$\chi(\omega)$ at K= 1/12, 3/12, 5/12, 7/12, 9/12, 11/12, for M=0.8μ_B. Strong Stoner excitations can be seen for K=1/12 and 3/12 near $\bar{\omega}$~10-20 meV. (**b**): Contours $|1-I\mathrm{Re}\chi_0|$ = 0 in the (ω,K) plane, for M=1.1μ_B and 0.8μ_B, analogous to Fig. 2(b), and dominant peak positions $\bar{\omega}$ obtained by a nonlinear least-squares fit of one or two gaussian functions to $\chi(\omega)$ over the region where peaks occur.

Along the FM line $\mathbf{q}$=(0,K,0)$2\pi/a$, $\chi(\omega)$ is more complex, and more difficult to interpret. At M=1.1μ_B sharp, well defined collective excitations are found at low q, and broaden with increasing q. There is a reasonably close correspondence with the zeros of $|1-I\mathrm{Re}\chi_0|$ and peaks in χ, as Fig. 3(b) shows. The M=0.8μ_B case is roughly similar, except that for K>0.4 excitations cannot be described by a single peak. Note that for fixed q, propagating spin fluctuations (characterized by peaks at $\bar{\omega}$) can exist at *multiple energies* — the magnetic analog of the dielectric function passing through zero and sustaining plasmons at multiple energies. Peaks in $\chi(\omega)$ can broaden as a consequence of this; the K=7/12, 9/12 and 11/12 data of Fig. 3(a) are broadened in part by this mechanism as distinct from the usual one (intermixing of Stoner excitations). Second, consider how $\partial\bar{\omega}/\partial q$ changes with M for K>0.5

(Fig. 3(b)). When M=1.1μ_B, $\bar{\omega}$ increases monotonically with K. For M=0.8μ_B, $\bar{\omega}$ has a complex structure but apparently reaches a maximum before K reaches 1. That $\partial\bar{\omega}/\partial q$ changes sign is significant: it marks the disappearance of magnetic frustration between the ferromagnetically aligned spins at low moments, and the emergence of stable FM order along [010], characteristic of local-moment behavior (see also Ref.[12]). Experimentally, Ref. [2] reports $\partial\bar{\omega}/\partial q$>0 for K>0.5. While our calculations provide a clear physical interpretation, we note significant differences in the moment where we observe this effect (M=0.8-1.1μ_B) and the effective spin (S=0.2) used in Ref.[2].

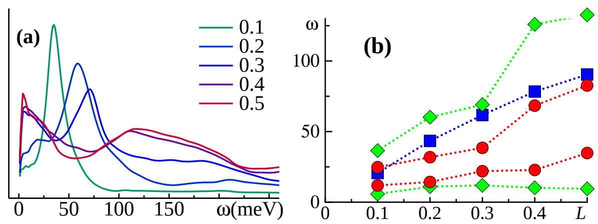

FIG. 4: Imχ($\mathbf{q}$,ω) along the c axis, $\mathbf{q}$=[0,0,L]$2\pi/c$. (**a**) Im$\chi(\omega)$ at values of L listed in the key, for M=0.8μ_B. When M=1.1μ_B (not shown) the spectrum is well characterized by a single sharp peak at any L. When M=0.8 or 0.4μ_B the SW peak remains, but a low-energy Stoner excitation coexists with it. The latter are most pronounced for larger L but can be resolved at every L. Peak positions (single for M=1.1μ_B, double for M=0.8 and 0.4μ_B) are shown in (**b**).

Elementary excitations along the c axis, $\mathbf{q}$=(0,0,L)$2\pi/c$, bring into highest relief the transition from pure local-moment behavior (collective excitations), to one where coherent itinerant Stoner and collective excitations coexist. Collective excitations are found for all L and all M. For M=1.1μ_B, a single peak is found: excitations are well described by the Heisenberg model with weak damping. Comparing Fig. 4(b) to Figs. 2(b) and 3(b), it is apparent that $\bar{\omega}$ rises much more slowly along L than along H or K, confirming that interplane interactions are weak. When M drops to 0.8μ_B, a second-low energy peak at $\bar{\omega}'$ emerges at energies below 20 meV, for small q along [0,K,0], and for all q along [0,0,L], coexisting with the collective excitation. Why these transitions are absent for M=1.1μ_B and are so strong at M=0.8μ_B can be understood in terms of roughly cylindrical Fermi surface at k=(1/2,0,k_z). Single spin-flip transitions between occupied states $\epsilon^{\uparrow}_{\mathbf{k}}$ and an unoccupied states $\epsilon^{\downarrow}_{\mathbf{k+q}}$ separated by ∼10 meV are responsible for this peak (see Eq. 2). They originate from "hot spots" where $N(\epsilon^{\uparrow}_{\mathbf{k}})$ and $N(\epsilon^{\downarrow}_{\mathbf{k+q}})$ are both large.

From the *SW velocities*, $(\partial\bar{\omega}/\partial q)_{q=0}$, anisotropy of the exchange couplings can be determined [4, 12, 14]. We find strong in-plane and out-of-plane anisotropies, and predict v_b/v_a=0.55 and find v_c/v_a=0.35, where v_a=490meV·Å. Neutron scattering experiments [14, 15] have measured with v_c/v_{a-b} to be ∼0.2-0.5.

In summary, we broadly confirm the experimental findings of Refs. [1, 2], that there is a spectrum of magnetic excitations of the striped phase of $CaFe_2As_2$, which for the most part are weakly damped at small q and more strongly damped at large q. A new kind of excitation was found, which originates from single particle-hole transitions within a narrow band of states near E_F, renormalized by a small denominator $|1 - I\mathrm{Re}\chi_0|$ (Eq. (1)). They appear when the Fe moment falls below a threshold, at which point the narrow band passes through E_F. The character of itineracy is novel: excitations occur at low-energy, at energy scales typically below T_N, and can be sharply peaked, which should make them accessible to experimental studies. The distinction between the two kinds of excitations is particularly observable in the anomalous dependence of $\Gamma/\bar{\omega}$ on q in Fig. 2(d). Collective spin-wave-like excitations also are unusual: multiple branches are found at some q. Finally, at higher q we find that the SW velocity changes sign, which is also observed experimentally at similar values of M.

Overall a picture emerges where localized and itinerant magnetic carriers coexist and influence each other. This description falls well outside the framework of a local-moments model such as the Heisenberg hamiltonian. The low-energy particle-hole excitations are strongly affected by Fe-As distance (and thus by lattice vibrations) while the SWs are much less so. While phonons and Stoner excitations are generally considered separately, these findings suggest that they strongly influence each other.

This work was supported by ONR, grant N00014-07-1-0479 and by DOE contract DE-FG02-06ER46302. Work at the Ames Laboratory was supported by DOE Basic Energy Sciences, Contract No. DE-AC02-07CH11358.

[1] S.O. Diallo et al., Phys. Rev. Lett. 102, 187206 (2009).

[2] J. Zhao et al., Nature Physics **5**, 555 (2009).

[3] M. D. Johannes, I.I. Mazin. Phys. Rev. B 79, 220510 (2009); I.I. Mazin, J. Schmalian. Physica

C, 469, 614 (2009).

[4] Z. P. Yin et al., Phys. Rev. Lett. **101**, 047001 (2008).

[5] Chen Fang et al., Phys. Rev. B 77, 224509 (2008); F. Kruger, S. Kumar, J. Zaanen and J. van den Brink. Phys. Rev.B 79, 054504 (2009); C. Lee, W. Lin and W. Ku. arXiv.0905.3782; R. R. P. Singh. arxiv.0903.4408.

[6] T. Kotani, M. van Schilfgaarde, S. V. Faleev, Phys. Rev. B**76**, 165106 (2007).

[7] T. Kotani and M. van Schilfgaarde, J. Phys. Cond. Matt. 20, 295214 (2008).

[8] R. Martin, *Electronic Structure*, Cambridge University Press (Cambridge, 2004).

[9] A.I. Goldman et al., Phys. Rev. B 78, 100506 (2008).

[10] N. Ni et al., Phys. Rev. B 80, 024511 (2009); E. D. Mun, S. L. Bud'ko, N. Ni, P. C. Canfield. arXiv:0906.1548.

[11] The origin of the discrepancy in $\bar{\omega}$ with experiment is not clear. Our calculation contains several important approximations (local potential, linear response, rigid spin).

[12] J J Pulikkoti et. al, Supercond. Sci. Technol. **23**, 054012 (2010).

[13] G. Samolyuk and V.P.Antropov. Phys. Rev. B 79, 052505 (2009).

[14] R. J. McQueeney et al., Phys. Rev. Lett. 101, 227205 (2008).

[15] J. W. Lynn and P. Dai. Physica C469, 469 (2009).